**Registry No.** ATP, 56-65-5; FITC, 27072-45-3; I, 20461-54-5; ATPase, 9000-83-3; Ca, 7440-70-2; vanadate, 37353-31-4; phosphate, 14265-44-2.

## References


Andersen, J. P., Moller, J. V., & Jorgensen, P. L. (1982) *J. Biol. Chem. 257*, 8300–8307.

Ando, T., Duke, J. A., Tonomura, Y., & Morales, M. F. (1982) *Biochem. Biophys. Res. Commun. 109*, 1–6.

Clore, G. M., Gronenborn, A. M., Mitchinson, C., & Green, N. M. (1982) *Eur. J. Biochem. 128*, 113–117.

Coll, R. J., & Murphy, A. J. (1984) *J. Biol. Chem. 259*, 14249–14254.

Csermely, P., & Martonosi, A. (1985) *Biophys. J. 47*, 457a.

de Meis, L. (1981) *The Sarcoplasmic Reticulum*, Wiley-Interscience, New York.

de Meis, L., Martins, O. B., & Alves, E. W. (1980) *Biochemistry 19*, 4252–4261.

Eftink, M. R., & Ghiron, C. A. (1977) *Biochemistry 16*, 5546–5551.

Eletr, S., & Inesi, G. (1972) *Biochim. Biophys. Acta 282*, 174–179.

Hasselbach, W., & Oetliker, H. (1983) *Annu. Rev. Physiol. 45*, 325–339.

Highsmith, S. (1984) *Biochem. Biophys. Res. Commun. 124*, 183–189.

Highsmith, S., & Murphy, A. J. (1984) *J. Biol. Chem. 259*, 14651–14656.

Highsmith, S., Barker, D., & Scales, D. (1985) *Biochim. Biophys. Acta 817*, 123–133.

Inesi, G. (1981) *Cell Muscle Motil. 1*, 63–97.

Kurtenbach, E., & Verjovski-Almeida, S. (1985) *J. Biol. Chem. 260*, 9636–9641.

Lehrer, S. S. (1971) *Biochemistry 10*, 3254–3263.

Leonardt, H., Gordon, L., & Livingston, R. (1971) *J. Phys. Chem. 75*, 245–249.

MacLennan, D. H., Brandl, C. J., Korczak, B., & Green, N. M. (1985) *Nature (London) 316*, 696–700.

Martin, M., & Lindqvist, L. (1975) *J. Lumin. 10*, 381–390.

Mitchinson, C., Wilderspin, A. F., Trinnaman, B. J., & Green, N. M. (1982) *FEBS Lett. 146*, 87–92.

Morales, M. F., & Botts, J. (1979) *Proc. Natl. Acad. Sci. U.S.A. 76*, 3857–3859.

Murphy, A. J. (1981) *J. Biol. Chem. 256*, 12046–12050.

Nakamoto, R. K., & Inesi, G. (1984) *J. Biol. Chem. 259*, 2961–2970.

Parker, C. A., & Rees, W. T. (1960) *Analyst (London) 85*, 587–593.

Pick, U. (1981) *Eur. J. Biochem. 121*, 187–195.

Pick, U. (1982) *J. Biol. Chem. 257*, 6111–6119.

Pick, U., & Bassilian, S. (1981) *FEBS Lett. 123*, 127–130.

Scott, T. (1984) *Biophys. J. 47*, 3a.

Stahl, N., & Jencks, W. P. (1984) *Biochemistry 23*, 5389–5392.

Tanford, C. (1983) *Annu. Rev. Biochem. 52*, 379–409.

Torgerson, P. (1984) *Biochemistry 23*, 3002–3007.

Vaughan, W. M., & Weber, G. (1970) *Biochemistry 9*, 464–473.

Wells, J. A., & Young, R. G. (1980) *Biochemistry 19*, 1711–1717.


# Direct NMR Evidence That Prolidase Is Specific for the Trans Isomer of Imidodipeptide Substrates†


Glenn F. King, Carl R. Middlehurst, and Philip W. Kuchel*

*Department of Biochemistry, University of Sydney, Sydney, N.S.W., Australia 2006*


*Received July 3, 1985*


ABSTRACT: The in vitro hydrolysis by porcine kidney prolidase of the imidodipeptide L-alanyl-L-proline was monitored by using $^1H$ high-resolution NMR spectroscopy. The dipeptide exists as an equilibrium mixture of isomers with cis or trans conformation about the peptide bond. The $^{13}C$ and $^1H$ NMR spectra of the dipeptide displayed well-resolved resonances for each isomer. Inversion-transfer NMR spectroscopy, with a recently developed pulse sequence, was used with a range of temperatures to calculate the unitary rate constants for the exchange between isomers. A new analytical procedure was introduced for directly obtaining estimates of the unitary rate constants from inversion-transfer data. Arrhenius analysis yielded an activation energy for the isomerization of 87.0 ± 4.1 kJ $mol^{-1}$. $^1H$ NMR time courses of the prolidase-catalyzed hydrolysis of L-alanyl-L-proline showed a faster removal of the trans isomer as the [enzyme]/[substrate] ratio was increased. The transient-kinetic information coupled with the steady-state kinetic parameters of the enzyme was used to develop two possible models of the overall hydrolytic reaction. Numerical integration of the relevant differential equations using the experimentally determined rate constants gave simulated progress curves that enabled selection of one of the proposed schemes as being the most likely; this proposal entailed absolute specificity of prolidase for the trans isomer of L-alanyl-L-proline. Finally, on the basis of the present work, and information from the literature, we have proposed a new model of the active site of the enzyme.


Prolidase (proline dipeptidase; EC 3.4.13.9) is a highly specific exopeptidase, cleaving only those dipeptides with a C-terminal proline or hydroxyproline residue. The enzyme is anatomically ubiquitous in man and other animals, having been characterized from brain (Hui & Lajtha, 1978), erythrocytes (Endo et al., 1982), heart (Smith, 1948), intestinal mucosa (Rubino et al., 1969), kidney (Davis & Smith, 1957), leukocytes (Powell et al., 1974), liver (Norên et al., 1977),

†This work was supported by a grant from the Australian National Health and Medical Research Council. G.F.K. gratefully acknowledges the support of a Commonwealth Postgraduate Research Award.

0006-2960/86/0425-1054$01.50/0 

plasma (Myara et al., 1984a), skin fibroblasts (Sheffield et al., 1977), thymus (Fruton et al., 1948), and the uterus (Smith, 1948). A rare congenital abnormality in man known as prolidase deficiency, in which there is a complete absence of the enzyme, manifests itself as a general clinical syndrome which includes splenomegaly, chronic ulcerative dermatitis, recurrent respiratory tract infection, mild to moderately severe mental retardation, and massive imidodipeptiduria [for a review, see Kaloustian et al. (1982)].

Despite numerous investigations on the substrate specificity of prolidase, there is a paucity of detailed kinetic information on the enzyme; this may in part be due to the tedious chemical procedure used for its assay (Myara et al., 1982). The necessity for more detailed information on the kinetics and mechanism of prolidase is emphasized by the inability to correlate many of the clinical manifestations of generalized prolidase deficiency with any of the known functions of the enzyme; not surprisingly, most attempts at clinical treatment of the enzyme deficiency have proven unsuccessful (Myara et al., 1984b).

The prolidase-catalyzed reaction is kinetically complicated because its imidodipeptide substrates generally exist as a mixture of cis and trans isomers due to the presence of the proline residue. For example, the percentage of the cis isomer, under physiological conditions, may vary from ~75% for L-phenylalanyl-L-proline to ~35% for glycyl-L-proline (Grathwohl & Wüthrich, 1976). Only one study so far has addressed the question of the specificity of prolidase with respect to the two possible isomeric forms of its substrate (Lin & Brandts, 1979). This latter work indicated that, when prolidase activity was high compared with substrate concentrations, reaction-progress curves could be separated into two distinct kinetic phases, with the second phase being considerably slower than the first. By using two different substrates in different ionic states, it was shown that the ratio of the percentage of reaction completed during the fast phase to that completed during the slow phase closely approximated the trans/cis ratio of the dipeptide, while the rate and activation energy of the slow phase were similar to the values for cis to trans isomerization of the substrate. The authors proposed that this was indirect evidence that prolidase is absolutely specific for the trans form of its substrate; the fast phase was inferred to be due to rapid hydrolysis of the trans isomer while the slow phase was due to rate-limiting cis to trans isomerization once the trans form had been totally hydrolyzed.

In the present work, we showed unequivocally that prolidase is absolutely specific for the trans isomer of its substrates; this was achieved by direct observation using $^1$H NMR spectroscopy of all chemical species in the prolidase-catalyzed hydrolysis of L-alanyl-L-proline. The work combined the known ability of NMR to observe cis and trans isomers of prolyl peptides (Deslauriers & Smith, 1980) and to monitor the prolidase reaction (King & Kuchel, 1984; Middlehurst et al., 1984). We also demonstrated that the rates of cis–trans isomerization of imidodipeptides can be measured under constant conditions [unlike the pH-jump method of Brandts et al. (1975)] using NMR magnetization-transfer techniques.

## Materials and Methods

*Materials.* Sodium 4,4-dimethyl-4-silapentane-1-sulfonate (DSS) was obtained from Aldrich Chemical Co., Milwaukee, WI. L-Alanyl-L-proline (Ala-Pro) and porcine kidney prolidase (lot 53F-0217) were purchased from Sigma Chemical Co., St. Louis, MO. The enzyme was obtained as a crystalline suspension (7.5 mg of protein mL$^{-1}$) in 2.7 M $(NH_4)_2SO_4$, pH 8.0, and had a specific activity of ~265 units/mg of protein; one unit will hydrolyze 1.0 μmol of glycyl-L-proline/min at pH 8.0 and 37 °C. Other chemicals were analytical reagent grade.

*General NMR Procedures.* $^{13}$C and $^1$H NMR spectra were recorded at 100.6 and 400 MHz, respectively, by using a Bruker WM400 spectrometer operating in the pulsed Fourier transform mode. Probe temperatures were calibrated by using the ethylene glycol method of Kaplan et al. (1975).

*Measurement of Cis–Trans Isomerization Rates.* The inversion-transfer pulse sequence recently described by Robinson et al. (1985) was used to measure the cis–trans isomerization rates of Ala-Pro at high temperatures. The pulse sequence is

$$\pi/2_x-\tau_1-\pi/2_{\pm x}-\tau_2-\pi/2_{\pm x,\pm y}-\text{acquisition}$$

where $\tau_1 = 1/2\Delta\nu$, $\Delta\nu$ is the chemical shift difference in hertz between the resonances of the two species (A and B) undergoing exchange, and $\tau_2$ is a variable delay time which generally extends from the lowest delay period available on the spectrometer to greater than 5 times the $T_1$ of the noninverted resonance. The subscripts $\pm x$ and $\pm y$ refer to the rotating frame axes along which the radio-frequency irradiation is applied. The spectrometer frequency is set to the resonance frequency of the species (B) whose magnetization is to be "inverted". Thus, at the end of the $\tau_1$ delay, the B magnetization lies along the positive $y$ axis in the rotating frame while the A magnetization is diametrically opposed. The second $\pi/2$ pulse aligns the magnetizations along the $z$ axis, with the B magnetization negative. The rate of exchange of inverted B spins can be calculated by measuring the amplitude (intensity) of the A and/or B resonances as a function of the variable delay time $\tau_2$ (see Theory). In the present experiments, $\Delta\nu$ was 36.6 Hz, and thus, $\tau_1$ was 13.65 ms. To avoid analytical complications caused by dephasing of the high- and low-frequency components of the cis and trans alanyl $\beta$-$CH_3$ doublets during the period $\tau_1$, they were collapsed to singlets by selective irradiation of the cis and trans alanyl $\alpha$-CH resonances. Inversion-transfer experiments generally employed 16–20 $\tau_2$ values, and 8–24 transients were normally averaged into 8192 data locations for each spectrum; 0.5-mL samples of Ala-Pro (450–500 mM) in 100 mM sodium phosphate buffer (final pH 7.8) were used for these measurements. $T_1$ values were measured by using the inversion-recovery pulse sequence (Farrar & Becker, 1971).

*Prolidase Time Courses.* $^1$H NMR time courses of the prolidase-catalyzed hydrolysis of Ala-Pro were obtained as follows: 7–35 μL of prolidase was added to a volume of 100 mM sodium phosphate buffer, pH 8.0, sufficient to bring the total volume to 450 μL, in a 5-mm-o.d. NMR tube. The buffer also contained 5 μM $MnSO_4$; $Mn^{2+}$ is an allosteric activator of prolidase but is not essential for activity (Myara et al., 1982). Although enzyme activity can be stimulated 3-fold by preincubation for 24 h with 0.9 mM $Mn^{2+}$ (Myara et al., 1982), this was not possible here as divalent manganese is paramagnetic and at millimolar concentrations it leads to relaxation broadening of NMR resonances (Conlon & Outhred, 1972). Furthermore, assuming 100% purity of the enzyme preparation, the concentration of $Mn^{2+}$ used here was sufficient to be equimolar with prolidase even at the highest enzyme concentration; the enzyme was also incubated with the buffer for 24 h prior to NMR experiments. Time courses were initiated by the addition of 50 μL of Ala-Pro (99.7 mM) constituted in the same buffer; this was taken as zero reaction time. The sample was then lowered into the probe, and spectral acquisition was normally begun within 1.5 min.

Spectra of 32–128 transients each, averaged into 8192 data

locations, were then acquired. The pulse sequence was simply a $\pi/2$ pulse preceded by 85 ms of selective irradiation at the resonance frequency of water and with homodecoupling at the predetermined frequency of the alanine $\alpha$-CH resonance during the acquisition period; this latter step improved spectral resolution between the $\beta$-$CH_3$ resonances of Ala-Pro and alanine by collapsing the latter to a sharp singlet (see Figure 5). For a spectral width of 5 kHz, the repetition time was 0.9042 s; spectra were thus acquired every 0.48–1.93 min.

## Theory

The quantitative application of NMR spin-transfer techniques to the measurement of rates of fast chemical exchange in systems at equilibrium was first developed by Forsén and Hoffman (1963, 1964); these authors showed that the time dependence of the nuclear magnetizations of two species undergoing exchange could be described by solving the Bloch equations that were previously modified to incorporate the effects of chemical exchange (McConnell, 1958). For the isomerization equilibrium under study here, viz.

$$\underset{\text{(cis Ala-Pro)}}{\text{A}} \underset{k_{-1}}{\overset{k_1}{\rightleftharpoons}} \underset{\text{(trans Ala-Pro)}}{\text{B}}$$

the modified Bloch equations are readily solved by the Laplace–Carson operator method (Kuchel, 1985) to yield equations which describe the time dependence of the nuclear magnetizations ($M_Z^A$ and $M_Z^B$) during the inversion-transfer experiment (Robinson et al., 1984):

$$M_Z^A(t) = M_E^A - M_0^A[\phi_1 \exp(-\lambda_1 t) + \phi_2 \exp(-\lambda_2 t)] \quad (1)$$

$$M_Z^B(t) = M_E^B - M_0^B[\phi_3 \exp(-\lambda_1 t) + \phi_4 \exp(-\lambda_2 t)] \quad (2)$$

where $\lambda_1$, $\lambda_2$, $\phi_1$, ..., $\phi_4$ are defined in the latter reference. The equilibrium rate constants can thus be experimentally determined by using the relationships:

$$k_{-1} = \frac{\lambda_1 + \lambda_2 - 1/T_1^A - 1/T_1^B}{1 + K_e} \quad (3)$$

$$K_e = [B]_e/[A]_e = k_1/k_{-1} \quad (4)$$

If the B resonance is inverted in the inversion-transfer experiment, then $\lambda_1$ and $\lambda_2$ are normally estimated by nonlinear least-squares regression of eq 1 onto the $M_Z^A$ vs. time data; this has more "character" (i.e., a minimum critical point) than the $M_Z^B$ vs. time curve. Initial estimates of $\lambda_1$ and $\lambda_2$ (which usually are required to be close to the true value to ensure convergence to a solution) are normally obtained by exponential peeling (Kuchel, 1985) of the data. A far more convenient method was derived by noting that as the $M_Z^A$ curve passes through its minimum value, the following expression applies:

$$\frac{dM_Z}{dt} = -\frac{M_Z^A - M_E^A}{T_1^A} - k_1 M_Z^A + k_{-1} M_Z^B = 0 \quad (5)$$

Rearranging this equation, and using eq 4, yields

$$k_{-1} = \frac{M_Z^A - M_E^A}{T_1^A(M_Z^B - K_e M_Z^A)} \quad (6)$$

Since $K_e$ and $T_1^A$ are known from other experiments, then $k_{-1}$ (and thus $k_1$) can be estimated by using the values of $M_Z^A$ and $M_Z^B$ when $M_Z^A$ is a minimum; $M_E^A$ is the value of $M_Z^A$ at the longest experimental time. By use of these values of $k_1$ and $k_{-1}$, accurate initial estimates of $\lambda_1$ and $\lambda_2$ can be calculated for the nonlinear regression procedure.

*Numerical Methods.* Equation 1 was fitted by using a nonlinear regression program (Miller, 1981) to inversion transfer experimental data consisting of the amplitude of the trans alanyl $\beta$-$CH_3$ resonance of Ala-Pro vs. variable delay time ($\tau_2$). Standard deviations of estimates of the unitary rate constants were calculated from those of the fitted parameters by using the general expression for the variance of a nonlinear function of several variables (Kendall & Stuart, 1977).

Numerical integration for the prolidase simulations was performed by using the program BIOSSIM (Roman & Garfinkel, 1978). This program converts the chemical reaction scheme of a given model into the corresponding set of differential equations and solves them by using an advanced predictor–corrector integration algorithm (Gear, 1971). A CYBER 825 computer was used for both numerical procedures.

Weighted linear regression of the transformed Arrhenius equation, viz.

$$\ln k = \ln [A] - E_a/RT \quad (7)$$

onto ln $k$ vs. $1/T$ data was performed on a Tektronix 4052 graphics computer programmed in BASIC, using $(k_i/\sigma_{k_i})^2$ as weights, where $k_i$ is the rate constant at the $i$th temperature and $\sigma_{k_i}$ is its standard deviation (Roberts, 1977).

## Results

Numerous $^{13}C$ NMR investigations have revealed that the cis–trans isomerism of peptides containing a proline residue manifests itself as different chemical shifts of the prolyl carbons of the cis and trans isomers, with the prolyl $\beta$- and $\gamma$-carbon resonances being particularly sensitive to the isomeric state of the peptide; the most detailed study has been by Grathwohl and Wüthrich (1976). However, as evident in the $^{13}C$ NMR spectrum of Ala-Pro (Figure 1A), the chemical shifts of the alanyl $\alpha$- and $\beta$-carbons are also sensitive to the orientation of groups around the peptide bond. Therefore, it is not surprising that the alanyl $\alpha$-CH and $\beta$-$CH_3$ resonances in the $^1H$ NMR spectrum of Ala-Pro (Figure 1B) have different chemical shifts for each isomer. The equilibrium constant ($K_e$) calculated from the ratio of the amplitudes (or intensities) of the alanyl $\beta$-$CH_3$ resonances in the $^1H$ NMR spectrum was the same as that calculated by using the ratio of the amplitudes (or intensities) of the prolyl $\beta$-carbon resonances in the $^{13}C$ NMR spectrum recorded at the same temperature. [Note that $K_e$ is temperature dependent; e.g., see Balaram et al. (1982).] Thus, it is possible to measure the rate of cis–trans isomerization of Ala-Pro in an inversion-transfer experiment by monitoring magnetization transfer between the alanyl $\beta$-$CH_3$ resonances; an equivalent $^{13}C$ NMR experiment using the prolyl $\beta$- or $\gamma$-carbon resonances would take considerably longer due to the reduced receptivity of the $^{13}C$ nuclei (thus requiring more transients per spectrum) and smaller $1/T_1$ relaxation rates (thus longer repetition times compared to $^1H$ spectra). For the reasons explained previously, the alanyl $\alpha$-CH resonances were selectively saturated during inversion-transfer experiments; an example is shown in Figure 1C.

The results of a typical inversion-transfer experiment performed at 351.9 K, with selective inversion of the cis alanyl $\beta$-$CH_3$ resonance, are given in Figure 2. The trans alanyl $\beta$-$CH_3$ resonance was reduced to a minimum of ~45% of its equilibrium amplitude due to exchange with inverted cis alanyl $\beta$-$CH_3$ spins before both resonances returned to equilibrium as a result of spin–lattice relaxation. In all, inversion-transfer experiments were performed at six different temperatures ranging from 336.9 to 354.4 K; the value of $K_e$ varied from 1.20 to 0.90 over this temperature range. Spin-transfer

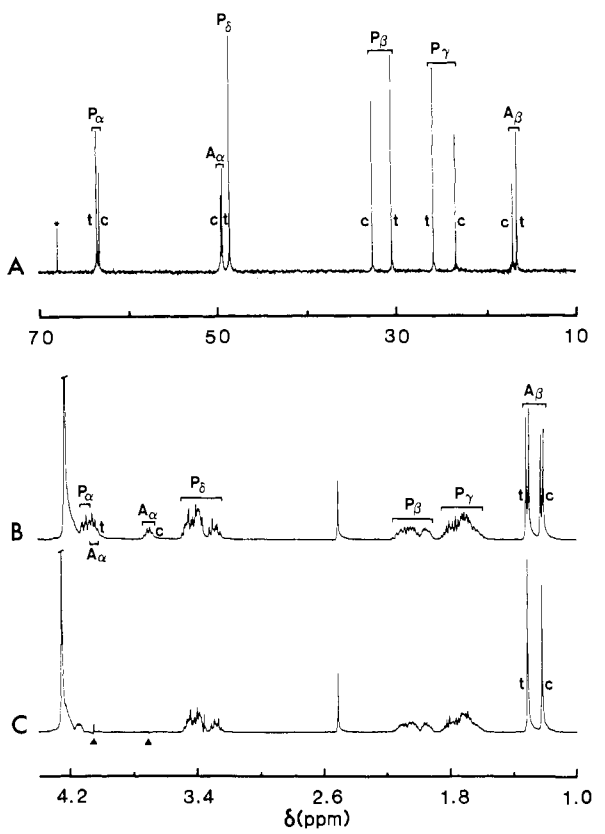


FIGURE 1: $^{13}C$ and $^{1}H$ NMR spectra of Ala-Pro. (A) $^{13}C$ NMR spectrum (128 transients in 16K data locations, obtained with broad-band proton decoupling) of a solution of Ala-Pro (475 mM in $D_2O$; pH 7.8) acquired at 310.0 K; (B) $^{1}H$ NMR spectrum (128 transients in 8K data locations) of a solution of Ala-Pro (466 mM in $D_2O$; pH 7.8) acquired at 336.9 K; (C) same as for (B) but with saturation of the trans and cis $A_\alpha$ resonances by irradiation at the frequencies indicated by (▲). Resonance assignments are given on the spectra (P denotes prolyl and A alanyl) with the resonances corresponding to the cis (c) and trans (t) conformations marked.

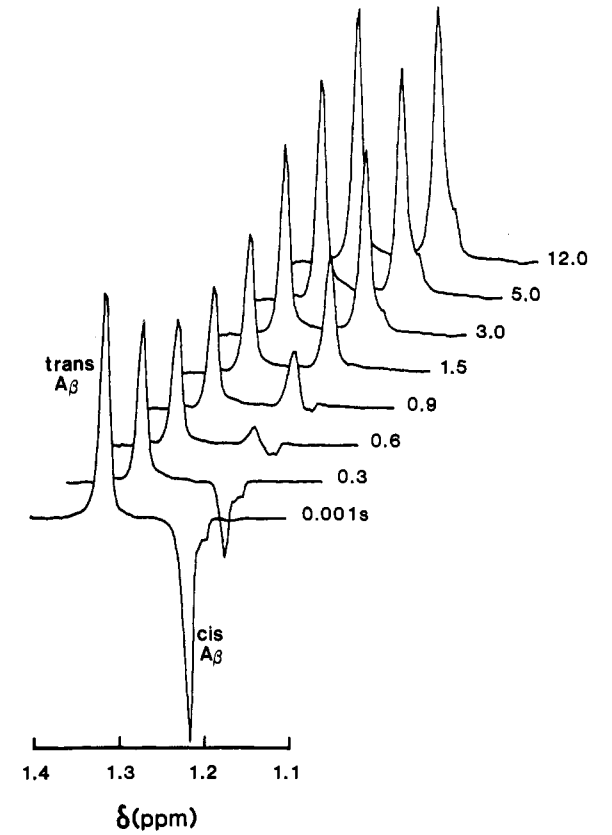


FIGURE 2: Series of $^{1}H$ NMR spectra (16 transients in 8K data locations) from an inversion-transfer experiment performed on Ala-Pro (466 mM in $D_2O$; pH 7.8) at a probe temperature of 351.9 K. The pulse sequence described in the text was used with spectrometer frequency (cis $A_\beta$) = 6134.23 Hz and $\tau_1$ = 13.65 ms. The variable delay time ($\tau_2$) is at the right of each spectrum. The small shoulder on the low-frequency side of the cis $A_\beta$ resonance is an unidentified impurity.

techniques are only applicable to kinetic systems where the rate constants and spin–lattice relaxation rates are of comparable magnitude; for Ala-Pro, this condition does not hold below ~330 K, with the result that its rate of isomerization can only be measured by this method at higher temperatures.

In Figure 3, the amplitude of the trans alanyl $\beta$-$CH_3$ resonance is plotted as a function of the variable delay time $\tau_2$ for two inversion-transfer experiments performed at the highest and lowest temperatures used in this work. The amplitudes were normalized to 1.0 at $\tau_2 = 0$ s for both temperatures. The solid curves were obtained by nonlinear least-squares regression of eq 1 onto the experimental data. The values of $\lambda_1$ and $\lambda_2$ were subsequently combined with $T_1$ and $K_e$ values to calculate $k_1$ and $k_{-1}$ using eq 3 and 4; this yielded $k_1 = 1.17 \pm 0.07$ s$^{-1}$ and $0.27 \pm 0.12$ s$^{-1}$ at temperatures of 354.4 and 336.9 K, respectively.

An Arrhenius plot using the $k_1$ values obtained at all six temperatures is shown in Figure 4. Weighted linear regression of eq 7 onto the transformed data yielded an estimate of the activation energy ($E_a$) for the cis–trans isomerization of Ala-Pro of $87.0 \pm 4.1$ kJ mol$^{-1}$, with a preexponential factor ($A$) of $7.51 \times 10^{12}$. In the Arrhenius plot, the error in ln $k_1$ is equal to $\sigma_{k_1}/k_1$ [i.e., for $y = f(x)$, $\delta y \sim f'(x)\delta x$]. Consequently, due to the data having a relatively constant variance, the error in ln $k_1$ becomes larger at lower temperatures.

Figure 5 shows $^{1}H$ NMR time courses of the hydrolysis of Ala-Pro by various concentrations of porcine kidney prolidase. All reactions were studied at 296.5 K for direct comparison

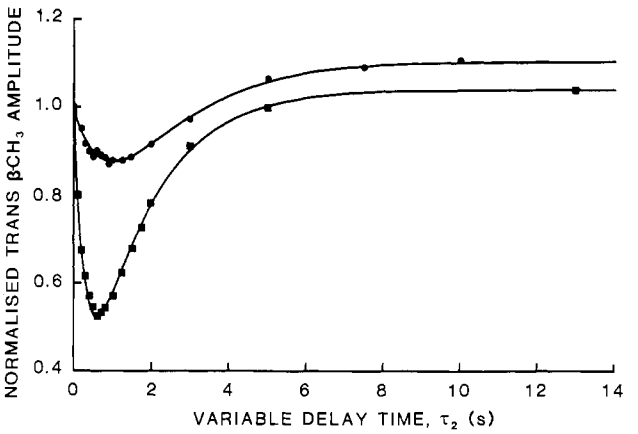


FIGURE 3: Plots of the trans $A_\beta$ magnetization (after inversion of the cis $A_\beta$ magnetization) vs. variable delay time ($\tau_2$) at 336.9 (●) and 354.4 K (■); the trans $A_\beta$ amplitude was normalized to be 1.0 at the lowest value of $\tau_2$. The solid curves were obtained by nonlinear least-squares regression of eq 1 onto the data; parameter values for the 336.9 K data were $\phi_1 = 0.82 \pm 0.46$, $\phi_2 = 0.71 \pm 0.46$, $\lambda_1 = 0.55 \pm 0.11$, and $\lambda_2 = 1.09 \pm 0.25$, and those for the 354.4 K data were $\phi_1 = -0.96 \pm 0.04$, $\phi_2 = 0.92 \pm 0.04$, $\lambda_1 = 0.640 \pm 0.026$, and $\lambda_2 = 3.14 \pm 0.15$.

with the previous work of Lin and Brandts (1979); similar results were obtained at 302.5 and 310.0 K (spectra not shown), but the reactions were considerably more rapid and required faster spectral acquisition (i.e., less transients), resulting in a lower signal to noise ratio. Note from Figure 5 that adequate spectral resolution between the cis and trans alanyl and alanine $\beta$-$CH_3$ resonances was achieved at all times.

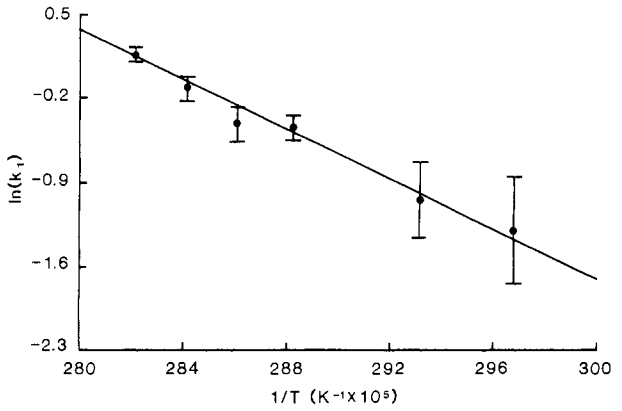


FIGURE 4: Arrhenius plot for the cis–trans isomerization of Ala-Pro as measured by using $^1$H NMR inversion-transfer spectroscopy. The solid line was obtained by weighted linear regression of eq 7 onto the data; this yielded estimates of the activation energy (87.0 ± 4.1 kJ mol$^{-1}$) and the preexponential factor ($A$; 7.51 × $10^{12}$).

Consequently, the concentrations of cis Ala-Pro (C), trans Ala-Pro (T), and free alanine (A) were determined at all reaction times as follows: From the principle of conservation of mass, we note that

$$[C] + [T] + [A] = [S]_0 \quad (8)$$

where the brackets denote molar concentrations and $[S]_0$ is the *total* initial concentration of Ala-Pro (i.e., both isomers). Integration of the modified Bloch equation, which relates the concentration of a species to its NMR signal intensity (Abragam, 1961), reveals that the peak amplitude of a given species is proportional to its concentration in the sample. Equation 8 can thus be expressed in the form:

$$\epsilon_c C + \epsilon_T T + \epsilon_A A = [S]_0 \quad (9)$$

where $C$, $T$, and $A$ are the peak amplitudes of the cis alanyl, trans alanyl, and alanine $\beta$-$CH_3$ resonances, respectively, and $\epsilon_C$, $\epsilon_T$, and $\epsilon_A$ are the corresponding NMR extinction coefficients. It may be intuitively expected that $\epsilon_C$ would equal $\epsilon_T$ (since it is envisaged that the cis and trans isomers of Ala-Pro would be very similar in terms of molecular dimensions and movements). Experimentally, this was verified by measuring these parameters at nine different temperatures; the mean difference in the values of $\epsilon_C$ and $\epsilon_T$ at each temperature was only 4%. Thus, we can simplify eq 9 to

$$\epsilon_C(C + T) + \epsilon_A A = [S]_0 \quad (10)$$

Rearranging eq 10, we obtain

$$C + T = -(\epsilon_A/\epsilon_C)A + [S]_0/\epsilon_C \quad (11)$$

Simple regression of a straight line ($y = mx + b$) onto $C + T$ vs. $A$ data yielded the best-fit NMR extinction coefficients and thus enabled the concentrations of all species to be calculated. For example, from the experiment depicted in Figure 5B, it was determined by this method that $\epsilon_C$ (=$\epsilon_T$) = 0.635 and $\epsilon_A$ = 0.515. This method is superior to calculating concentrations by using calibration curves, since the latter assumes a unique set of extinction coefficients, which may in fact vary from one experiment to another due to variations in paramagnetic impurities, local field inhomogeneities, etc. Figure 6 shows the concentration vs. time curves for cis Ala-Pro, trans Ala-Pro, and alanine calculated by using the peak amplitudes of the $\beta$-$CH_3$ resonances of these species in the time courses shown in Figure 5. The origin of the solid curves in Figure 6 is discussed below.

## Discussion

The only authors to have previously reported rate constants for the cis–trans isomerization of prolyl peptides in aqueous solution (Brandts et al., 1975; Lin & Brandts, 1979) exploited the difference in the carboxyl group p$K_a$ of the cis and trans isomers; the lower p$K_a$ of the cis isomer (Evans & Rabenstein, 1974) manifests itself as an increasing proportion of the trans form as the pH is lowered. For example, the trans/cis ratio for Ala-Pro may increase from ~1.5 to ~9.0 as the pH is lowered from 6.5 to 1.5 (Grathwohl & Wüthrich, 1976). Thus, Brandts and co-workers were able to calculate the cis–trans isomerization rates of Gly-Pro, Ala-Pro, Val-Pro, and Phe-Pro by "jumping" the dipeptides to a new pH and measuring the unique relaxation times.

Unfortunately, the only measurements of activation energies for the isomerization reactions were obtained from experiments in which the final pH of the solution was 3.5; the rate constants obtained may thus only be applicable at pH 3.5 since activated-complex theory (Atkins, 1978) states that the rate will be dependent on the pH and ionic strength of the medium. In fact, the ionic strength dependence of the rate constants for cis–trans isomerization was demonstrated by Brandts et al. (1975), and the pH dependence is given in Table II of the paper by Lin and Brandts (1979). In view of this, we decided that, for use in the simulations of the prolidase-catalyzed reaction (see later), it was desirable to determine accurate rate

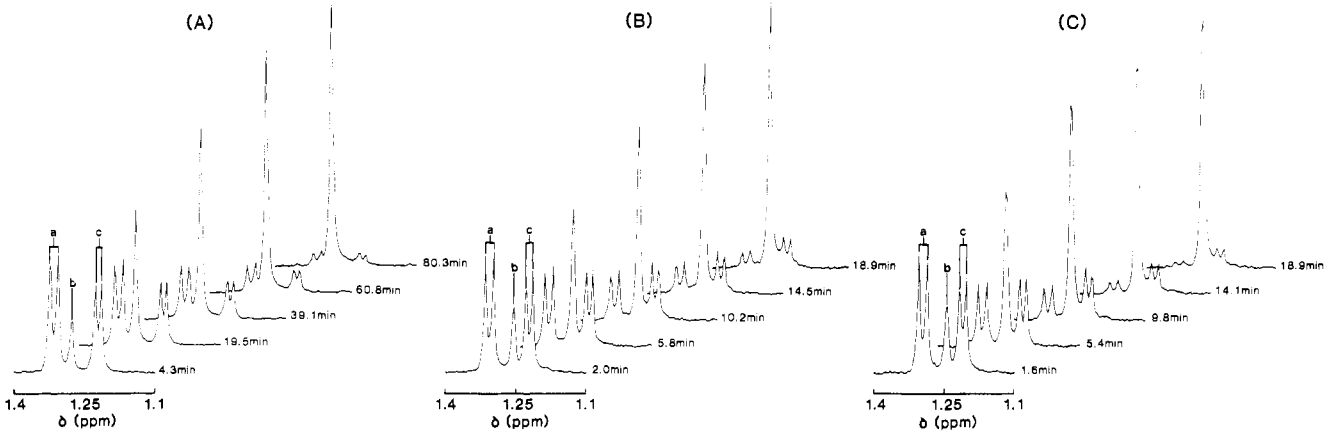


FIGURE 5: $^1$H NMR time courses of the prolidase-catalyzed hydrolysis of Ala-Pro (9.97 mM). Experimental conditions are explained in the text; the ratios of prolidase activity to substrate concentration, with the volume of prolidase added to the incubation mixture given in parentheses, were (A) 2.8 units/μmol (7 μL), (B) 10.8 units/μmol (27 μL), and (C) 14.0 units/μmol (35 μL). $^1$H NMR spectra were acquired into 8K data locations using 144 transients per spectrum for (A) and 32 transients per spectrum for (B) and (C). Spectral assignments are as follows: a, trans $A_\beta$ of Ala-Pro; b, decoupled $A_\beta$ of alanine; c, cis $A_\beta$ of Ala-Pro.

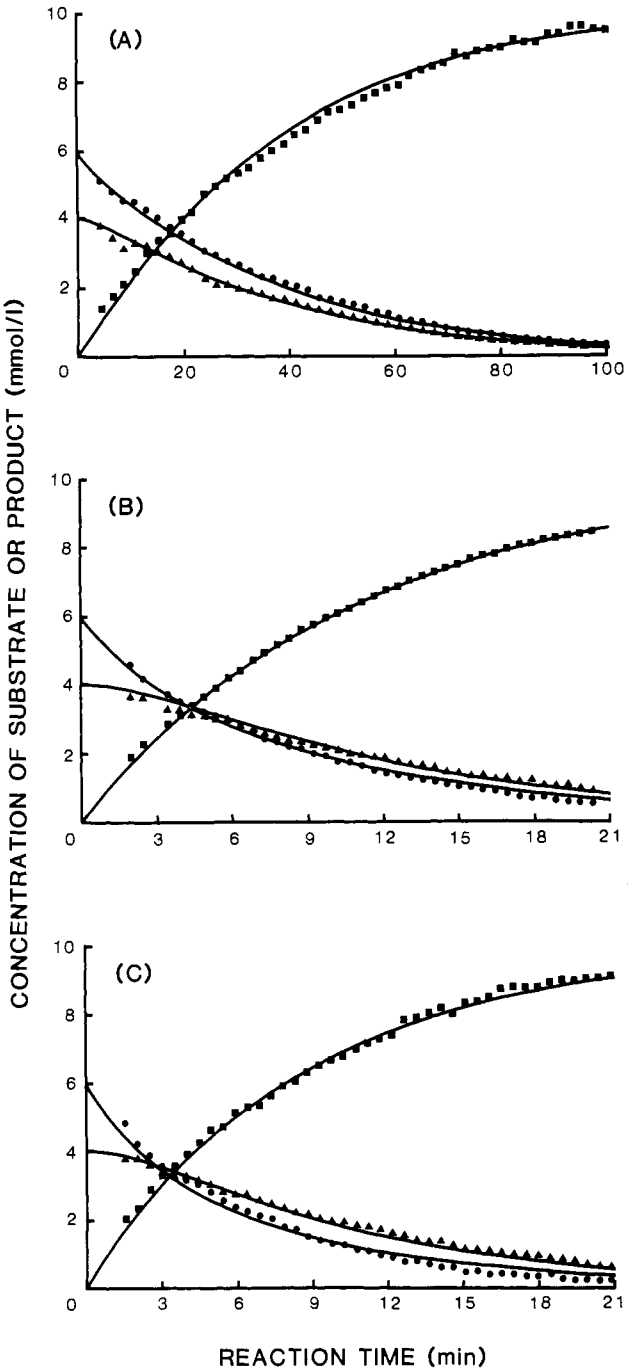


FIGURE 6: (A–C) Progress curves derived from the $^1$H NMR time courses depicted in Figure 5A–C, respectively. The various chemical species are (●) trans Ala-Pro, (▲) cis Ala-Pro, and (■) alanine. The solid curves in (A) represent the best visual fit obtained by numerical integration of the differential equations obtained by using Scheme I (see text). The unitary rate constants pertaining to this scheme were as follows: $k_1$, $3.54 \times 10^{-3}$ s$^{-1}$; $k_{-1}$, $2.37 \times 10^{-3}$ s$^{-1}$; $k_2$, $1.00 \times 10^6$ L mol$^{-1}$ s$^{-1}$; $k_{-2}$, $1.50 \times 10^4$ s$^{-1}$; $k_3$, 34.2 s$^{-1}$. The initial concentrations of the various species were as follows: trans Ala-Pro, $5.97 \times 10^{-3}$ mol L$^{-1}$; cis Ala-Pro, $4.00 \times 10^{-3}$ mol L$^{-1}$ (i.e., $K_e = 1.49$); prolidase, $4.25 \times 10^{-7}$ mol L$^{-1}$. The solid curves in (B) and (C) represent the numerical simulations obtained by using the same unitary rate constants and initial conditions as for (A), except that the prolidase concentration was altered according to the additional volume of prolidase used in each of the corresponding $^1$H NMR experiments.

constants for the cis–trans isomerization of Ala-Pro at the pH optimum of the porcine kidney enzyme (pH 7.8–8.0). We demonstrated that NMR inversion-transfer techniques could be used to monitor the rate of isomerization, under constant conditions, at temperatures above 335 K. At pH 7.8, we

Scheme I

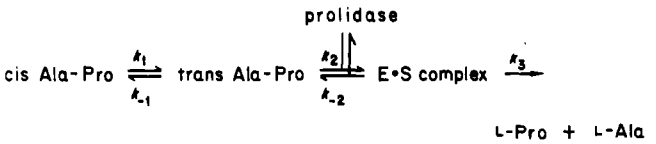


Scheme II

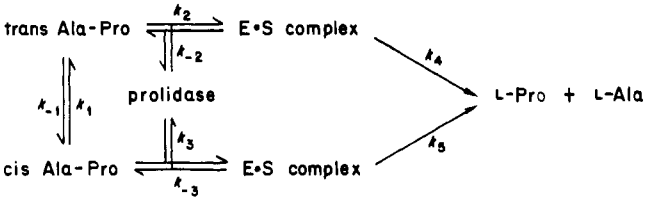


obtained an activation energy for the isomerization process of 87.0 ± 4.1 kJ mol$^{-1}$ compared to the value of 82.8 kJ mol$^{-1}$ (19800 cal) obtained previously by Brandts et al. (1975) from the pH-jump experiments. The values of $k_1$ (the rate constant for isomerization in the cis to trans direction) at 296.5 K, predicted by this study and that of Brandts et al. (1975), are $3.54 \times 10^{-3}$ and $3.73 \times 10^{-3}$ s$^{-1}$, respectively. Our value was used in all computer simulations of the prolidase reaction reported here. Since $K_e$ was found to be 1.49 at 296.5 K and pH 7.8, $k_2$ was calculated to be $2.37 \times 10^{-3}$ s$^{-1}$.

It is clear from the experimental progress curves depicting the prolidase-catalyzed hydrolysis of Ala-Pro (Figure 6) that the trans isomer is removed more rapidly than the cis isomer as the enzyme/substrate ratio is increased. Two possible models of the prolidase reaction could account for this observation: (1) prolidase may be absolutely specific for the trans isomer of Ala-Pro; thus, as the enzyme/substrate ratio is increased, the rate of cis–trans isomerization would become more rate limiting and the trans isomer would be consumed increasingly more rapidly than the cis isomer. The final phase of the reaction would be solely dependent on, and thus equal to, the rate of isomerization of the cis isomer. This model is designated Scheme I. (2) Prolidase may be capable of hydrolyzing both isomers of Ala-Pro, but the trans isomer is a more "efficient" substrate (i.e., higher $V_{max}$ and/or lower $K_m$). This model is designated Scheme II.

In order to decide which model best represented the prolidase reaction, we attempted to fit the simulation of a particular model to the experimental data in Figure 6A to obtain estimates of the unitary rate constants; $k_1$ and $k_{-1}$ were set to the values calculated from the inversion-transfer data. To test the model, the relevant differential equations were solved numerically to simulate the experiments relating to Figure 6B, C. Let us first consider Scheme I. The differential rate equations for both schemes are nonlinear, and consequently, analytical expressions for the concentration of each species as a function of time cannot be obtained. Therefore, the unitary rate constants for Scheme I were estimated by using visual comparisons of numerically simulated time courses with the experimental data; for the numerical integrations, $k_1$ and $k_{-1}$ were held constant at their predetermined values, and all "on" rate constants were set equal to $1.00 \times 10^6$ mol$^{-1}$ L s$^{-1}$. The maximal flux through the enzyme ($V_{max}$) in the simulation shown in Figure 6A was varied by changing $k_3$ and assuming a constant prolidase concentration of 0.425 μM (calculated by using an arbitrary value of ~45% purity for the commercially prepared enzyme and a prolidase molecular weight of 108 000; Sjöström & Norén, 1974).

The solid lines in Figure 6A represent the best, visually determined, correspondence of the numerical integration of

Table I: Relative Activities of Prolidase with Various Substrates and Some Properties of These Substrates

| substrate (X-Pro) | length of side chain (Å)[a] | % of substrate in trans form[b] | cis → trans rate constant ($min^{-1}$)[c] | rel act. with prolidase from | |
|---|---|---|---|---|---|
| | | | | porcine intestine[f] | calf brain[g] |
| Ala | 3.3 | 60 | 0.19[d] | 100 | 100 |
| Ser | 4.8 | | | 90 | |
| Met | 7.9 | | | 40 | |
| Gly | 2.3 | 63 | 0.16[e] | 30 | 37 |
| Glu | 6.8 | | | 30 | |
| Leu | 6.1 | 51 | | | 22 |
| Phe | 7.4 | 24 | 0.023[e] | | 5 |
| Pro | 4.2 | | | 0 | 0 |

[a] Calculated as the extended chain length, including the van der Waals radius of the terminal atom. The operational "chain length" will depend on the solution-conformation of the imidodipeptide. [b] pH 6.5, 298 K; Grathwohl & Wüthrich (1976). [c] Calculated for 295.5 K. [d] Data from the present work. [e] Lin & Brandts (1979). [f] pH 6.8, 298 K; Sjöström et al. (1973). [g] Hui & Lajtha (1978).

Scheme I and the experimental data. The unitary rate constants are given in the legend; they yielded values of $K_m$ and $V_{max}$ for trans Ala-Pro of 15.0 mmol $L^{-1}$ and 0.435 μmol/min, respectively. The solid lines in Figure 6B, C are numerical simulations of time courses using the same unitary rate constants and concentrations as the simulation in Figure 6A except that the prolidase concentration was altered according to the additional volume of prolidase used in these experiments. It can be seen that the latter two "predicted" time courses are in excellent agreement with the experimental data. Therefore, under the range of experimental conditions tested here, Scheme I is an accurate representation of the prolidase reaction.

Attempts to fit the experimental data in Figure 6A by using numerical simulations of Scheme II were unsuccessful; reasonable fits could only be obtained if the $K_m$ of the cis isomer was unrealistically large and the $V_{max}$ approached a value 50 times less than that of the trans isomer, i.e., the reaction reduced to that of Scheme I. Thus, we concur with Lin and Brandts (1979) that porcine kidney prolidase has exceptionally high, or absolute, specificity for the trans isomer of its imidodipeptide substrates. The immediate implication of this result is that all previous steady-state kinetic studies on purified prolidase, which failed to consider the isomeric specificity of the enzyme, must be reevaluated. Since these studies used initial velocity analyses, the "true" $K_m$ (for the trans isomer) may be simply obtained by multiplying the reported value by the fractional amount of substrate which exists as the trans isomer. The recalculated $K_m$ values (in millimoles per liter) assuming $K_e$ = 1.5 for both Ala-Pro and Gly-Pro are as follows: porcine kidney/Gly-Pro (Manao et al., 1972), 2.8; monkey intestine/Gly-Pro (Baksi & Radhkrishnan, 1974), 3.6; calf brain/Ala-Pro (Hui & Lajtha, 1980), 12.00. Note that the corrected $K_m$ value for calf-brain prolidase with Ala-Pro as substrate is very similar to the value of 15.0 mmol $L^{-1}$ reported here for the porcine kidney enzyme.

In view of prolidase being absolutely specific for the trans isomer of its substrates, it is possible to revise the proposed configuration of the active site of prolidase (Figure 7A; Hui & Lajtha, 1978). The important characteristics of their proposed active site were (i) an ionic interaction between the prolyl carboxyl and a site on the enzyme, (ii) an adjacent hydrophilic pocket to which the proline pyrrolidine ring binds, (iii) a $Mn^{2+}$ binding site which enables polarization of the peptide-bond carbonyl group, making it more susceptible to hydrolysis, (iv) an ionic interaction between the N-terminus and the enzyme, and (v) a pocket binding the side chain of the N-terminal amino acid. Note that in this proposed model the $Mn^{2+}$ and prolyl-carboxyl binding sites are positioned on opposite sides of the peptide bond, allowing only the cis isomer to enter the active site; however, the all-trans mechanism of the prolidase reaction implies that these groups should be

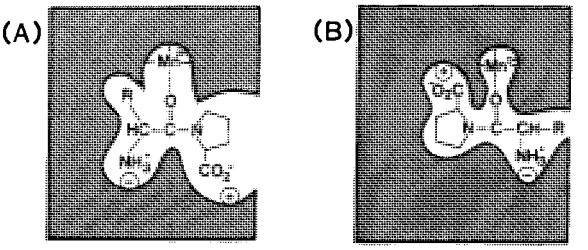


FIGURE 7: (A) Hypothetical active site of prolidase as proposed by Hui and Lajtha (1978); (B) revised active-site model for prolidase. See text for explanation; the hatched area represents the enzyme.

positioned on the same side of the peptide bond so only the trans isomer can bind.

Furthermore, Hui and Lajtha (1978) claimed that the main determinant of the substrate specificity of prolidase was the pocket binding the side chain of the N-terminal amino acid; they proposed that this was quite rigid with a depth of 2.5 Å since imidodipeptides in which the length of the N-terminal amino acid side chain was greater than 2.5 Å were "poor" substrates. However, the relative activities of prolidase toward various substrates suggest a more subtle determinant of prolidase substrate specificity; these data are summarized in Table I together with the relative proportions of the substrate in the trans form, the rates of cis–trans isomerization, and the length of the N-terminal amino acid side chain. It should be noted that the imidodipeptide cis/trans ratios reported in Table I (Grathwohl & Wüthrich, 1976; pH 6.5, 298 K) will be nearly identical with those found under the assay conditions used in the substrate specificity studies (Sjöström et al., 1973; pH 6.8, 298 K); the only difference in conditions between these studies, 0.3 pH unit, is not significant as $K_e$ varies negligibly over the pH range 5.0–7.5 (this study, data not shown). The substrate specificities recently reported for purified human erythrocyte prolidase (Endo et al., 1982) have been excluded from Table I because they are in conflict with most other substrate specificity data for prolidase; the specificities also differ from those determined for the human erythrocyte enzyme in situ (King & Kuchel, 1984; Vandenberg et al., 1985). It is clear from Table I (columns 2, 5, and 6) that side-chain length correlates poorly with relative enzymatic activity; a much better correlation exists, despite the paucity of data, between the percentage of the substrate which exists as the trans isomer (column 3) and the rate of cis–trans isomerization (column 4). That is, those imidodipeptides with a large proportion of the trans isomer and a fast rate of cis–trans isomerization tend to be "good" substrates for prolidase. In other words, this is a reflection of the absolute specificity of prolidase toward the trans isomer.

Consequently, in order to explain the basis of prolidase specificity, there is no need to propose a rigid pocket of limited

size for the side chain of the N-terminal amino acid. Furthermore, Hui and Lajtha (1978) proposed that this hypothetical pocket must be nonpolar or uncharged polar, since charged imidodipeptides are, they claimed, "poor" prolidase substrates. However, the high activity of porcine intestinal prolidase toward Glu-Pro (Table I, column 5) and the ability of bovine plasma prolidase to hydrolyze His-Pro (Ganapathy et al., 1982) provide two counter examples that lead us to refute their proposal. A prolidase active site which is more compatible with the variety of data available on the enzyme is shown in Figure 7B. The main characteristics of this newly proposed site are the following: (i) cationic and anionic binding sites for the C- and N-termini, respectively (activity toward the substrates is abolished if either the N- or the C-termini are blocked; Adams & Smith, 1952); (ii) a pocket to bind the pyrrolidine ring; (iii) a binding site for $Mn^{2+}$ oriented such that the peptide-bond carbonyl can only be polarized if the imidodipeptide is in the trans conformation, i.e., the $Mn^{2+}$ binding site must be on the same side of the peptide bond as the C-terminus binding site; and (iv) no specific binding site for the side chain of the N-terminal amino acid. The orientation of the binding site for the N-terminus with respect to the $Mn^{2+}$ binding site is unclear, but its stereochemistry is assumed to be important; addition of an extra carbon between the carbonyl group and the $\alpha$-carbon of the N-terminus, as in $\beta$-alanyl-L-proline, abolishes the susceptibility of the peptide bond to hydrolysis (Adams & Smith, 1952).

It is anticipated that additional investigations will add to the data in Table I and lead to a better understanding of the mechanism of the prolidase reaction; this may give insight into the physiological functions of the enzyme and the basis of the symptomatology of generalized prolidase deficiency.

## ACKNOWLEDGMENTS

Dr. B. E. Chapman is thanked for acquiring the $^{13}C$ NMR spectra, and Dr. G. L. Mendz, Dr. J. E. Gready, and G. Robinson are thanked for valuable discussions. B. T. Bulliman and W. G. Lowe provided expert computing and technical assistance, respectively.

**Registry No.** Ala-Pro, 13485-59-1; prolidase, 9025-32-5.

## REFERENCES

Abragam, A. (1961) in *The Principles of Nuclear Magnetism*, Oxford University Press, Oxford.

Adams, E., & Smith, E. L. (1952) *J. Biol. Chem. 198*, 671–682.

Atkins, P. W. (1978) in *Physical Chemistry*, pp 897–925, Oxford University Press, Oxford.

Baksi, M., & Radhkrishnan, A. N. (1974) *Indian J. Biochem. Biophys. 11*, 7–11.

Balaram, H., Venkataram Prasad, B. V., & Balaram, P. (1982) *Biochem. Biophys. Res. Commun. 109*, 825–831.

Brandts, J. F., Halvorson, H. R., & Brennan, M. (1975) *Biochemistry 14*, 4953–4963.

Conlon, T., & Outhred, R. (1972) *Biochim. Biophys. Acta 288*, 354–361.

Davis, N. C., & Smith, E. L. (1957) *J. Biol. Chem. 224*, 261–275.

Deslauriers, R., & Smith, I. C. P. (1980) in *Biological Magnetic Resonance* (Berliner, L. J., & Reuben, J., Eds) Vol. II, pp 275–280, Plenum Press, New York.

Endo, F., Matsuda, I., Ogata, A., & Tanaka, S. (1982) *Pediatr. Res. 16*, 227–231.

Evans, C. A., & Rabenstein, D. L. (1974) *J. Am. Chem. Soc. 96*, 7312–7317.

Farrar, T. C., & Becker, E. D. (1971) *Pulse and Fourier Transform NMR: Introduction to Theory and Methods*, Academic Press, New York.

Forsén, S., & Hoffman, R. A. (1963) *J. Chem. Phys. 39*, 2892–2901.

Forsén, S., & Hoffman, R. A. (1964) *J. Chem. Phys. 40*, 1189–1196.

Fruton, J. S., Smith, V. A., & Driscoll, P. E. (1948) *J. Biol. Chem. 173*, 457–469.

Ganapathy, V., Fonteles, M., Pashley, D. H., & Leibach, F. H. (1982) *Biochim. Biophys. Acta 719*, 154–157.

Grathwohl, C., & Wüthrich, K. (1976) *Biopolymers 15*, 2025–2041.

Hui, K. S., & Lajtha, A. (1978) *J. Neurochem. 30*, 321–327.

Hui, K. S., & Lajtha, A. (1980) *J. Neurochem. 35*, 489–494.

Kaloustian, V. M. D., Freij, B. J., & Kurvan, A. K. (1982) *Dermatologica 164*, 293–304.

Kaplan, M. L., Bovey, F. A., & Cheng, H. N. (1975) *Anal. Chem. 47*, 1703–1705.

Kendall, M., & Stuart, A. (1977) *The Advanced Theory of Statistics*, Vol. 1, pp 243–262, Charles Griffin, London.

King, G. F., & Kuchel, P. W. (1984) *Biochem. J. 220*, 553–560.

Kuchel, P. W. (1985) in *Catalytic Facilitation in Organized Multienzyme Systems* (Welch, G. R., Ed.) pp 303–380, Academic Press, New York.

Lin, L. N., & Brandts, J. F. (1979) *Biochemistry 18*, 43–47.

Manao, G., Nassi, P., Cappugi, G., Canici, G., & Ramponi, G. (1972) *Physiol. Chem. Phys. 4*, 75–87.

McConnell, H. M. (1958) *J. Chem. Phys. 28*, 430–431.

Middlehurst, C. R., King, G. F., Beilharz, G. R., Hunt, G. E., Johnson, G. F. S., & Kuchel, P. W. (1984) *J. Neurochem. 43*, 1561–1567.

Miller, A. J. (1981) Consulting Report No. Vt 81/23, C.S. I.R.O. Division of Mathematics and Statistics, South Melbourne, Australia.

Myara, I., Charpentier, C., & Lemonnier, A. (1982) *Clin. Chim. Acta 125*, 193–205.

Myara, I., Myara, A., Mangeot, M., Fabre, M., Charpentier, C., & Lemonnier, A. (1984a) *Clin. Chem. (Winston-Salem, N.C.) 30*, 211–215.

Myara, I., Charpentier, C., & Lemonnier, A. (1984b) *Life Sci. 34*, 1985–1998.

Norén, O., Dabelsteen, D., Sjöström, H., & Josefsson, L. (1977) *Gastroenterology 72*, 87–92.

Osborne, M. R. (1976) *J. Austr. Math. Soc. B 19*, 343–357.

Powell, G. F., Rasco, A., & Maniscalo, R. M. (1974) *Metab. Clin. Exp. 23*, 505–513.

Roberts, D. V. (1977) *Enzyme Kinetics*, pp 292–295, Cambridge University Press, Cambridge.

Robinson, G., Chapman, B. E., & Kuchel, P. W. (1984) *Eur. J. Biochem. 143*, 643–649.

Robinson, G., Kuchel, P. W., Chapman, B. E., Doddrell, D. M., & Irving, M. G. (1985) *J. Magn. Reson. 63*, 314–319.

Roman, G.-C., & Garfinkel, D. (1978) *Comput. Biomed. Res. 11*, 3–15.

Rubino, A., Pierro, M., La Torretta, G., Vetrella, M., Di Martino, D., & Autrichhio, S. (1969) *Pediatr. Res. 3*, 313–319.

Sheffield, L. J., Schlesinger, P., Faull, K., Halpern, B. J., Schier, G. M., Cotton, R. G. H., Hammond, D. J., &

Danks, D. M. (1977) *J. Pediatr. 91*, 578–583.
Sjöström, H., & Norén, O. (1974) *Biochim. Biophys. Acta 359*, 177–185.
Sjöström, H., Norén, O., & Josefsson, L. (1973) *Biochim. Biophys. Acta 327*, 457–470.
Smith, E. L. (1948) *J. Biol. Chem. 173*, 553–569.
Vandenberg, J. I., King, G. F., & Kuchel, P. W. (1985) *Biochim. Biophys. Acta 846*, 127–134.

# Sterol Orientations in Phosphatidylcholine Liposomes As Determined by Deuterium NMR†

Ramaswamy Murari,‡ Martha P. Murari,§ and Wolfgang J. Baumann*
*Bio-Organic Chemistry Section, The Hormel Institute, University of Minnesota, Austin, Minnesota 55912*
*Received June 26, 1985*

ABSTRACT: Deuterium magnetic resonance spectra (55.26 MHz) of cholesterol-3α-$d_1$ and epicholesterol-3β-$d_1$ in dipalmitoylglycerophosphocholine (DPPC) liposomes were measured as a function of sterol-to-phospholipid ratio below (24 °C) and above (60 °C) the phase transition temperature of DPPC. From the quadrupolar splittings $\Delta\nu_q$, the molecular order parameters $S$ describing the motions of the sterols in the bilayer were calculated, and the most probable angle of tilt $\alpha_0$ of the molecular axis of the sterols relative to the bilayer normal was determined. We observed that the molecular axis of cholesterol in DPPC liposomes at both 24 and 60 °C is tilted at an angle of 16–19° with the 3β-hydroxyl group projecting parallel to the bilayer normal into the aqueous interface. In contrast, at 24 °C, epicholesterol is aligned parallel (0°) to the bilayer normal, placing the 3α-hydroxyl group essentially perpendicular to the bilayer normal along the aqueous interface. At 60 °C, the average angle of epicholesterol (16–18°) is similar to that of cholesterol, which can project the 3α-hydroxyl group into the hydrophobic bilayer region. On the basis of the observed tilt angles of the two isomeric sterols in DPPC liposomes, a *model* is proposed that can rationalize the differential effects of cholesterol and epicholesterol on membrane properties. The near-parallel alignment, at both 24 and 60 °C, of cholesterol relative to the fatty acyl chains in phospholipid bilayers (16–25°), with the sterol 3β-hydroxyl group projecting into the aqueous interface, would promote strong lipophilic interactions as well as hydration of the hydroxyl function. The nonparallel arrangement, at 24 °C, of epicholesterol and the fatty acyl chains, again assuming an acyl tilt of 16–25°, would reduce lipophilic interactions as compared to those observed for cholesterol, while the hydroxyl function would remain relatively accessible to hydration. At 60 °C, even though epicholesterol would be oriented nearly parallel to the acyl chains, effective lipophilic interactions as well as hydration would be hindered by the 3α-hydroxyl group rotating into the hydrophobic bilayer region. The differential sterol effects of cholesterol and epicholesterol are discussed in light of the model proposed.

Considerable research has focused on the effect of cholesterol on structural and dynamic membrane properties. However, there is still no satisfactory explanation for the unique role of cholesterol in modulating natural and model membranes [for a review, see Presti et al. (1982)]. By comparison, the α-hydroxyl isomeric epicholesterol exerts diminished effects on phospholipid membranes, reflecting greatly reduced sterol–phospholipid interactions (Demel et al., 1972a,b; Bittman & Blau, 1972; Silbert, 1975; Clejan et al., 1979).

Chart I


**1** CHOLESTEROL-3α-$d_1$, $R_1$ = OH, $R_2$ = $^2$H

**2** EPICHOLESTEROL-3β-$d_1$, $R_1$ = $^2$H, $R_2$ = OH

Attempts to rationalize the differential effects of the two isomeric sterols on the basis of stereospecific interactions between the sterol hydroxy function and specific phospholipid sites have not held up to experimental scrutiny. Thus, earlier studies had suggested (Darke et al., 1972; Verma & Wallach, 1973) that the β-hydroxyl group of cholesterol may specifically interact with the phosphatidylcholine (PC)[1] phosphate function in PC–cholesterol bilayers; yet, subsequent NMR studies have clearly ruled out this possibility (Keough et al., 1973; Stockton

† This study was supported in part by U.S. Public Health Service Research Grant HL 08214 from the Program Projects Branch, Extramural Programs, National Heart, Lung and Blood Institute, by NIH Training Grant HL 07311, by Research Grants CA 12150 and NS 14304, and by The Hormel Foundation. High-field $^2$H NMR measurements were done at the NSF Midwest Regional Instrumentation Facility, University of Illinois, Urbana (E. Oldfield, Director), supported by Grant CHE 79-16100. Preliminary results of this study were presented at the 23rd Experimental NMR Conference, Madison, WI, April 1982.
* Address correspondence to this author.
‡ Present address: Revlon Health Care, Research & Development Division, Tuckahoe, NY 10707.
§ Present address: Chemistry Department, Yale University, New Haven, CT 06511.

[1] Abbreviations: PC, phosphatidylcholine; DMPC, dimyristoylglycerophosphocholine; DPPC, dipalmitoylglycerophosphocholine; NMR, nuclear magnetic resonance; $Me_4Si$, tetramethylsilane; TLC, thin-layer chromatography; IR, infrared.

0006-2960/86/0425-1062$01.50/0 